
RANDOMIZED APPROACH TO MATRIX COMPLETION: APPLICATIONS IN COLLABORATIVE FILTERING AND IMAGE INPAINTING

Antonina Krajewska
 NASK National Research Institute
 Warsaw, Poland
 antonina.krajewska@nask.pl

Ewa Niewiadomska-Szynkiewicz
 Warsaw University of Technology
 Warsaw, Poland
 ewa.szynkiewicz@pw.edu.pl

ABSTRACT

We present a novel method for matrix completion, specifically designed for matrices where one dimension significantly exceeds the other. Our Columns Selected Matrix Completion (CSMC) method combines Column Subset Selection and Low-Rank Matrix Completion to efficiently reconstruct incomplete datasets. In each step, CSMC solves a convex optimization problem. We introduce two algorithms to implement CSMC, each tailored to problems of different sizes. A formal analysis is provided, outlining the necessary assumptions and the probability of obtaining a correct solution. To assess the impact of matrix size, rank, and the ratio of missing entries on solution quality and computation time, we conducted experiments on synthetic data. The method was also applied to two real-world problems: recommendation systems and image inpainting. Our results show that CSMC provides solutions of the same quality as state-of-the-art matrix completion algorithms based on convex optimization, while achieving significant reductions in computational runtime.

Keywords Matrix completion · Column Subset Selection · Low-rank models · Image inpainting · Collaborative filtering · Nuclear Norm · Convex Optimization

1 Introduction

Images, time series, and graphs are just a few examples of data types that can naturally be represented as real-valued matrices. In practice, these matrices often have missing entries due to data collection costs, sensor errors, or privacy considerations. To fully exploit the potential of matrix-based datasets, we need to address the missing data problem. Matrix completion (MC) methods leverage assumptions about underlying patterns in the data, which often manifest as a low-rank property of the matrix being analyzed. This low-rank characteristic reflects inherent correlations or regularities in the data, enabling effective recovery of missing entries.

Matrix completion has found applications in diverse fields such as signal processing, sensor localization, medicine and genomics [1–4]. Its significance was underscored by the Netflix Prize challenge, which focused on predicting unknown ratings using collaborative filtering based on the preferences of many users [5–7]. The task involves completing the sparse user-movie rating matrix $\mathbf{M} \in \mathbb{R}^{n_1 \times n_2}$, where n_1 (the number of users) is significantly larger than n_2 (the number of movies). This creates an imbalanced matrix in which most entries are missing, as users only rate a small subset of movies.

Singular Value Decomposition (SVD) forms the basis of many MC algorithms. It is commonly used to exploit the high correlation in the data by decomposing the matrix \mathbf{M} as follows:

$$\mathbf{M} = \mathbf{U}\Sigma\mathbf{V}^T, \quad (1)$$

where $\mathbf{U} \in \mathbb{R}^{n_1 \times n_1}$, $\mathbf{V} \in \mathbb{R}^{n_2 \times n_2}$ are orthogonal, and $\Sigma \in \mathbb{R}^{n_1 \times n_2}$ is non-negative diagonal matrix of singular values, ordered according to their magnitude. The singular values indicate the strength of the variance along the corresponding

directions, which are captured by the columns of \mathbf{U} and \mathbf{V} . The rank of \mathbf{M} is determined by the number of non-zero singular values. A common approach to MC is to identify the matrix of lowest rank that best approximates the observed entries. However, directly minimizing the rank is NP-hard [5, 8]. Instead, minimizing the nuclear norm, which is the sum of the singular values of the matrix, is often pursued [5]. Let $\Omega \subseteq \{1, \dots, n_1\} \times \{1, \dots, n_2\}$ be the set of indices of the known entries, the convex optimization problem for the exact MC has the following form

$$\begin{cases} \text{minimize} & \|\mathbf{X}\|_* \\ \text{s.t.} & \mathcal{R}_\Omega(\mathbf{X} - \mathbf{M}) = 0, \end{cases} \quad (2)$$

where $\|\mathbf{X}\|_*$ denotes nuclear norm of the decision variable \mathbf{X} , $\mathcal{R}_\Omega : \mathbb{R}^{n_1 \times n_2} \rightarrow \mathbb{R}^{n_1 \times n_2}$ sets all matrix elements to 0, except those in the Ω set, e.g.

$$\mathcal{R}_\Omega(\mathbf{X}) = \sum_{(i,j) \in \Omega} x_{ij} \mathbf{e}_i \mathbf{e}_j^T, \quad (3)$$

where \mathbf{e}_i denotes standard basis vector with 1 on the i -th coordinate and 0 elsewhere. Nuclear norm minimization is a widely adopted technique for low-rank matrix completion, known for its theoretical guarantees and empirical solid performance [5, 9, 10]. It can be solved in time polynomial time in the matrix dimension, using off-the-shelf Semidefinite Programming (SDP) solvers or tailored first-order methods [5, 8, 10]. However, in large-scale problems, solving these SDP programs, even with first-order methods, can be computationally challenging due to memory requirements [10].

This paper introduces a novel method for the low-rank matrix completion problem, which we call Columns Selected Matrix Completion (CSMC). The CSMC benefits from integrating two fields of modern linear algebra. In particular, it employs the Column Subset Selection (CSS) algorithm to reduce the size of the matrix completion problem. Recovering the most essential columns limits the computational costs of the matrix completion task. In the second stage, the recovered and previously known entries are used to recover \mathbf{M} by solving the standard least squares problem [11–13]. CSMC is particularly useful when one dimension of \mathbf{M} is much larger than the other, such as in the Netflix Prize scenario. The integration of the two approaches allows CSMC to decrease the computational cost of the convex matrix completion algorithms while maintaining their theoretical guarantees.

1.1 Notation and abbreviations

For a matrix $\mathbf{X} \in \mathbb{R}^{n_1 \times n_2}$ we denote by \mathbf{x}_i its i -th column, and by x_{ij} its (i, j) -th entry. Given the set of column indices $\mathcal{I} \in [n_2]$ we use $\mathbf{X}_{:, \mathcal{I}}$ to denote the column submatrix. We consider three types of matrix norms. The spectral norm of \mathbf{X} is denoted by $\|\mathbf{X}\|_2$. The Frobenius and the nuclear norm are denoted by $\|\mathbf{X}\|_F$ and $\|\mathbf{X}\|_*$ respectively. Table 1 contains essential symbols and acronyms.

Notation	Description
Ω	set of indices of the observed entries
\mathcal{R}_Ω	sampling operator (3)
\mathcal{I}	column indices for the column submatrix \mathbf{C}
$\mathbf{X}_{:, \mathcal{I}}$	column submatrix of \mathbf{X} indicated by \mathcal{I}
\mathbf{X}^\dagger	Moore-Penrose inverse of \mathbf{X}
ρ	percentage of sampled entries
α	percentage of sampled columns in the first stage
r	rank of \mathbf{M}
$\mu_0(\mathbf{M})$	the coherence parameter of \mathbf{M}
CSS	Column Subset Selection
CSMC	Columns Selected Matrix Completion
CSNN	Columns Selected Nuclear Norm minimization
CSPGD	Columns Selected Proximal Gradient Descent
NN	Nuclear Norm minimization
PGD	Proximal Gradient Descent
MF	Matrix Factorization

Table 1: Notation and abbreviations

1.2 Outline of the paper

The rest of the paper is organized as follows: Section 2 reviews related methods and presents our contribution. In Section 3, we present our method and provide formal analysis, particularly Theorem 3.2, which offers a lower bound on the probability of perfect reconstruction of the matrix, along with conditions on the minimum number of randomly selected columns and the minimum size of the sample of known elements of the reconstructed matrix that ensure achieving this estimate. Section 4 contains experimental results on synthetic and real datasets, confirming the effectiveness of the proposed method.

2 Related work and contribution

2.1 Low-rank matrix completion

The low-rank assumption is grounded in the observation that the real-world datasets inherently possess, or can be effectively approximated by, a low-rank matrix structure [10]. It plays a pivotal role in enhancing the efficiency of algorithms. The algorithms for the low-rank matrix completion typically leverage convex or non-convex optimization in Euclidean spaces [9, 14–19], or employ Riemannian optimization [20–23]. The convex methods are the most mature and have strong and well-understood theoretical guarantees. The nuclear norm relaxation draws inspiration from the success of compressed sensing [5, 8, 10, 24] in which ℓ_1 norm minimization is used to recover sparse signal instead of ℓ_0 norm. The matrix rank may be expressed as the ℓ_0 norm of the singular values vector σ , while the nuclear norm is defined as its ℓ_1 norm.

Another notable solution, alongside exact matrix completion (2), is presented by Mazumder et al. [15]. To address noisy data and prevent model overfitting, they consider a regularized optimization problem,

$$\underset{\mathbf{X}}{\text{minimize}} \frac{1}{2} \|\mathcal{R}_\Omega(\mathbf{X}) - \mathcal{R}_\Omega(\mathbf{M})\|_F^2 + \lambda \|\mathbf{X}\|_*, \quad (4)$$

where λ is a regularization parameter. The problem (4) benefits from the closed form of the proximal operator for the objective function given by Singular Value Thresholding (SVT) and can be solved with Proximal Gradient descent (PGD) and its modifications [15].

Another class of convex optimization techniques focuses on minimizing the Frobenius norm error for the observed entries while applying constraints on the nuclear norm. It can be solved using the Frank-Wolfe (conditional-gradient descent) algorithm [25]. Despite its low computational cost per iteration, the Frank-Wolfe algorithm exhibits slow convergence rates. Consequently, numerous efforts have been undertaken to develop optimized variants of the algorithm [26, 27].

The non-convex optimization methods aim to minimize least squares error on the observed entries while constraining the rank of the solution with Matrix Factorization (MF) [10, 28],

$$\min_{\mathbf{L} \in \mathbb{R}^{n_1 \times k}, \mathbf{R} \in \mathbb{R}^{n_2 \times k}} \frac{1}{2} \|\mathcal{R}_\Omega(\mathbf{M}) - \mathcal{R}_\Omega(\mathbf{L}\mathbf{R}^T)\|_F^2. \quad (5)$$

Chen and Chi [10] distinguish three classes of methods solving (5), Alternating Minimization, Gradient Descent and Singular Value Projection. For Alternating Minimization, Jain et al. [14] and Hardt [19] gave provable guarantees. However, these guarantees are worse in terms of coherence, rank and condition number of \mathbf{M} .

2.2 Column Subset Selection

Many commonly employed low-rank models, such as Principal Component Analysis (PCA), Singular Value Decomposition (SVD), and Nonnegative Matrix Factorization (NNMF) lack clear interpretability, leading to research on alternatives like CSS and CUR decomposition [29–34]. CSS provides low-rank representation using the column submatrix of the data matrix $\mathbf{M} \in \mathbb{R}^{n_1 \times n_2}$. Formally, given a matrix $\mathbf{M} \in \mathbb{R}^{n_1 \times n_2}$ and a positive integer d , CSS seeks for the column submatrix $\mathbf{C} \in \mathbb{R}^{n_1 \times d}$ such that

$$\|\mathbf{M} - P_C(\mathbf{M})\|_\varepsilon \quad (6)$$

is minimized over all possible $\binom{n_2}{d}$ choices for the matrix \mathbf{C} . Parameter $\xi \in \{2, F\}$, where $\xi = 2$ denotes the spectral and $\xi = F$ the Frobenius norm. Here,

$$P_C = \mathbf{C}\mathbf{C}^\dagger, \quad (7)$$

is the projection onto the d -dimensional space spanned by the columns \mathbf{C} and \mathbf{C}^\dagger denotes the Moore-Penrose pseudoinverse [35]. On the other hand, CUR decomposition explicitly selects a subset of columns and rows from the original matrix to construct the factorization [31, 32].

Extensive research focuses on fully-observed matrices, which may not be practical for real-world applications [29–34]. Several works provide comprehensive overviews of CUR decomposition methods. For instance, [32] offers a detailed characterization of various forms of CUR, while [36] reviews different sampling strategies employed to construct CUR decompositions. Bridging the research gap between CSS, CUR and matrix completion is a recently recognized challenge [37–40]. In this context, two important questions emerge. The first one is about selecting meaningful columns (or rows) from partially observed data and applying CSS and CUR in matrix completion algorithms. Our method benefits from the fact that under standard assumptions about matrix incoherence, a high-quality column subset can be obtained by randomly sampling each column [41]. However, in the case of the coherent matrices, Wang and Singh [37] propose active sampling to dynamically adjust column selection during the sampling process, albeit with increased computational complexity.

The application of CUR and CSS in MC tasks typically involves altering the sampling scheme to relax assumptions about the matrix or reduce sample complexity [38–40]. However, estimating leverage scores, a key requirement in these methods, poses a significant challenge [37].

Cai et al. [3] showcase the potential of CUR in low-rank matrix completion, introducing a novel sampling strategy called Cross-Concentrating Sampling (CCS) and a fast non-convex Iterative CUR Completion (ICURC) algorithm. However, CCS requires $\mathcal{O}(r^2 n \ln^2(n))$ observed entries, where $n = \max\{n_1, n_2\}$, which is a factor of r worse than the nuclear norm minimization-based approach. The optimization problem solved by ICURC imposes constraints on the rank of the matrix, thus introducing an additional parameter that requires tuning.

Our approach is related to the work of Xu et al., who presented CUR++, an algorithm for partially observed matrices [41]. It computes a low-rank approximation of the matrix based on randomly selected columns and rows, along with a subset of observed entries. However, the reconstruction procedure requires finding eigenvectors of the observed submatrices, which adds a computational burden.

2.3 Our contributions

This paper addresses the challenge of completing rectangular matrices by integrating principles from Column Subset Selection and Low-rank Matrix Completion. Our approach involves solving convex optimization problems. Our main contributions are as follows:

1. We introduce a two-staged matrix completion method, CSMC, dedicated to recovering rectangular matrices with one direction significantly larger than the other ($n_1 \ll n_2$). This structure is particularly well-suited for large-scale and asymmetrical data scenarios common in multi-source data integration tasks.
2. We offer a formal analysis, including Theorem 3.2, which establishes a lower bound on the probability of achieving perfect matrix reconstruction in the second stage of CSMC. This theorem contains necessary conditions regarding the minimum number of randomly selected columns ($d = \mathcal{O}(r \ln r)$) and the minimum sample size of known elements ($|\Omega| = \mathcal{O}(n_2 r \ln(n_2 r))$) required for accurate reconstruction of an incoherent matrix of rank r .
3. We develop two algorithms dedicated to problems of different sizes: Columns Selected Nuclear Norm (CSNN) and Columns Selected Proximal Gradient Descent (CSPGD).
4. We validate the CSMC method through numerical experiments on synthetic and real-world datasets, comparing its performance with matrix completion algorithms from the literature, specifically for recommendation systems and image inpainting.

3 Columns Selected Matrix Completion (CSMC) method overview

In the CSMC, the completion of the matrix $\mathbf{M} \in \mathbb{R}^{n_1 \times n_2}$ is divided into two stages. In the first stage, CSMC selects the subset of d columns and fills it with an established matrix completion algorithm. In the second stage, the least squares problem is solved. Each of the presented variants of the CSMC methods adopts the following procedure (Fig. 1).

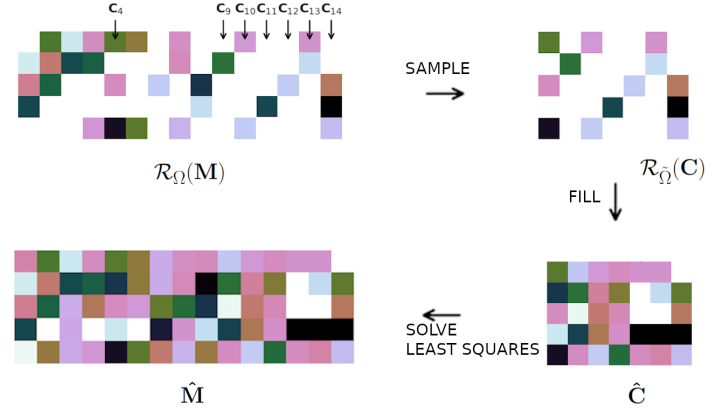


Figure 1: The CSMC method overview.

Stage I: Sample and fill

CSMC selects d columns of $\mathbf{M} \in \mathbb{R}^{n_1 \times n_2}$ according to the uniform distribution over the set of all indices. Let $I \subseteq \{1, \dots, n_2\}$ denote the set of the indices of the selected columns. The submatrix formed by selected columns, $\mathbf{C} := \mathbf{M}_{:,I}$, $\mathbf{C} \in \mathbb{R}^{n_1 \times d}$ is recovered using the chosen matrix completion algorithm.

Stage II: Solve least squares

Let $\hat{\mathbf{C}} \in \mathbb{R}^{n_1 \times d}$ be the output of the Stage I. The CSMC solves the following convex optimization problem,

$$\min_{\mathbf{Z} \in \mathbb{R}^{d \times n_2}} \frac{1}{2} \|\mathcal{R}_\Omega(\mathbf{M}) - \mathcal{R}_\Omega(\hat{\mathbf{C}}\mathbf{Z})\|_F^2, \quad (8)$$

where $\mathcal{R}_\Omega : \mathbb{R}^{n_1 \times n_2} \rightarrow \mathbb{R}^{n_1 \times n_2}$ is the sampling operator (eq. 3). Let $\hat{\mathbf{Z}} \in \mathbb{R}^{d \times n_2}$ be a solution to the problem (8). The CSMC output with the matrix $\hat{\mathbf{M}} = \hat{\mathbf{C}}\hat{\mathbf{Z}}$.

Algorithm 1 CSMC- α

```

Require:  $\mathcal{R}_\Omega(\mathbf{M})$ :  $n_1 \times n_2$ -matrix
Require:  $\alpha$ : Ratio of the selected columns
 $I \leftarrow$  Uniformly sample  $\alpha \cdot n_2$  indices
 $\mathbf{C}_{\text{missing}} \leftarrow \mathcal{R}_\Omega(\mathbf{M})_{:,I}$ 
 $\hat{\mathbf{C}} \leftarrow \text{MC}(\mathbf{C}_{\text{missing}})$  ▷ Complete submatrix  $\mathbf{C} \in \mathbb{R}^{n_1 \times d}$ .
 $\hat{\mathbf{Z}} \leftarrow \arg \min_{\mathbf{Z} \in \mathbb{R}^{n_2}} \frac{1}{2} \|\mathcal{R}_\Omega(\mathbf{M}) - \mathcal{R}_\Omega(\hat{\mathbf{C}}\mathbf{Z})\|_F^2$ 
 $\hat{\mathbf{M}} \leftarrow \hat{\mathbf{C}}\hat{\mathbf{Z}}$ 
return  $\hat{\mathbf{M}}$ 

```

3.1 Theoretical results

In their seminal work, Candes and Recht proved that, under certain assumptions, solving nuclear norm minimization leads to successful matrix recovery [17]. There has been a significant amount of research extending these results to noisy settings, improved bounds on the sample complexity and analyzing the robustness of the nuclear norm minimization algorithms to noise and outliers [5, 9, 18, 42]. Recht [9] greatly simplified the analysis and provided a foundation for understanding the potential and limitations of the method in practical matrix completion scenarios. The theoretical guarantees rely on properties such as matrix rank, number and distribution of observed entries and the fact that the singular vectors of the matrix are uncorrelated with the standard basis. The last property is formalized with the *matrix coherence* and defined as follows [17].

Definition 3.1. Let U be a subspace of \mathbb{R}^n of dimension r_U and P_U be the orthogonal projection onto U . The coherence parameter of U is defined as

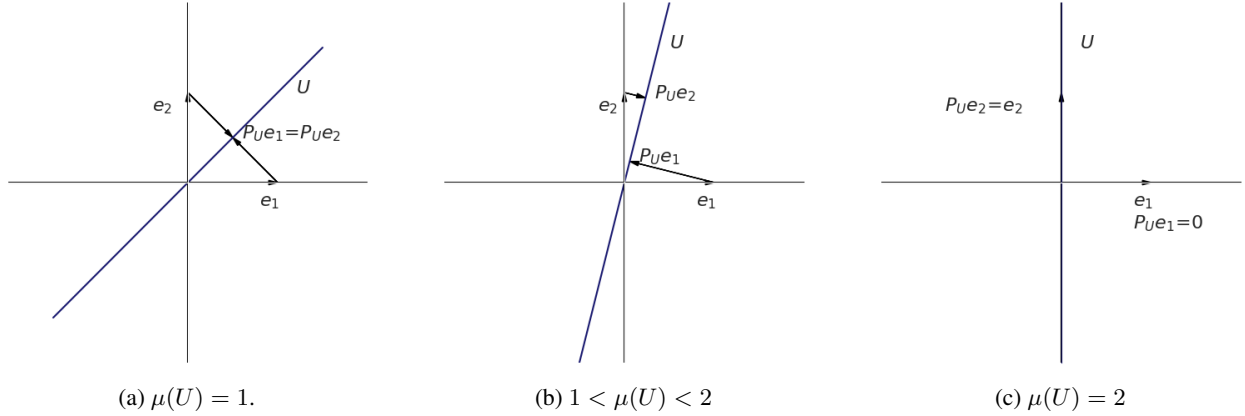


Figure 2: Coherence of the one-dimensional subspace $U \subset \mathbb{R}^2$: Fig. 2a depicts U , spanned by $(\frac{1}{\sqrt{2}}, \frac{1}{\sqrt{2}})$, with the smallest coherence $\mu(U) = 1$. Fig. 2b illustrates the case where $1 < \mu(U) < 2$, while Fig. 2c presents U , spanned by one of the standard basis vectors e_2 , which achieves maximal coherence $\mu(U) = 2$.

$$\mu(U) = \frac{n}{r_U} \max_{1 \leq i \leq n} \|P_U e_i\|_2^2, \quad (9)$$

where e_i for $i = 1, \dots, n$ are the standard basis vectors of \mathbb{R}^n .

The coherence parameter of the rank- \tilde{r} matrix \mathbf{X} is given by $\mu_0(\mathbf{X}) = \max\{\mu(U), \mu(V)\}$ where U and V are the linear spaces spanned by its \tilde{r} left and right singular vectors respectively.

We assume that observed entries are sampled uniformly at random. We begin with a discussion on how the crucial characteristics of the matrix \mathbf{M} completion problem are transferred to the task of filling in the submatrix \mathbf{C} . Since \mathbf{C} consists of randomly selected d columns of \mathbf{M} , the rank of \mathbf{C} is bounded by a minimum of r and d , and the entries of \mathbf{C} also follow a uniform distribution. The following theorem demonstrates that for an incoherent, well-conditioned matrix \mathbf{M} , if the submatrix \mathbf{C} is composed of $\mathcal{O}(r \ln(rn_2))$ sampled columns, it will exhibit low coherence.

Theorem 3.1 (Corollary 3.6 in Cai et al. [43]). *Suppose that $\mathbf{M} \in \mathbb{R}^{n_1 \times n_2}$ has rank r and coherence bounded by $\mu_0(\mathbf{M})$. Suppose that $I \subseteq \{1, \dots, n_2\}$ is chosen by sampling uniformly without replacement to yield $\mathbf{C} = \mathbf{M}_{:,I}$. Let d be the number of sampled columns such that $d \geq 1.06\mu_0(\mathbf{M})r \ln(rn_2)$. Then*

$$\mu_0(\mathbf{C}) \leq 100\kappa^2(\mathbf{M})\mu_0(\mathbf{M}), \quad (10)$$

with a probability at least $1 - \frac{1}{n_2}$, where $\kappa(\mathbf{M})$ denotes the spectral condition number of \mathbf{M} , given by $\kappa(\mathbf{M}) := \|\mathbf{M}\|_2 \|\mathbf{M}^\dagger\|_2$.

In this section, the primary focus lies on assessing the recovery capabilities of the least-squares problem during the second stage of the CSMC. In particular, we assume that submatrix \mathbf{C} is fully observed or perfectly recovered and provide assumptions that solving

$$\min_{\mathbf{Z} \in \mathbb{R}^{d \times n_2}} \frac{1}{2} \|\mathcal{R}_\Omega(\mathbf{M}) - \mathcal{R}_\Omega(\mathbf{C}\mathbf{Z})\|_F^2 \quad (11)$$

will output $\hat{\mathbf{Z}} \in \mathbb{R}^{d \times n_2}$, such that $\mathbf{M} = \mathbf{C}\hat{\mathbf{Z}}$ holds with high probability. While similar to the CUR+ framework introduced in [41], our approach to solving (11) avoids the need to compute singular vectors of \mathbf{C} . The main result of this section is given by the Theorem 3.2. We believe that the following main result broadens the result of Xu et al. formulated as Theorem 2 in [41]. The proof of Theorem 3.2 is provided in the appendix.

Theorem 3.2. *Let r be the rank of $\mathbf{M} \in \mathbb{R}^{n_1 \times n_2}$ and let $\mathbf{C} \in \mathbb{R}^{n_1 \times d}$ be a column submatrix of \mathbf{M} formed by uniformly sampled without replacement d columns. Let \tilde{r} denote the rank of \mathbf{C} . Assume that for the parameter $\gamma > 0$,*

1. $d \geq 7\mu_0(\mathbf{M})r(\gamma + \ln r)$,

$$2. |\Omega| \geq \tilde{r}n_2\mu_0(\mathbf{C}) \left(\gamma + \ln \left(\frac{n_2\tilde{r}}{2} \right) \right).$$

Let $\hat{\mathbf{Z}} \in \mathbb{R}^{d \times n_2}$ be the minimizer of the problem 11. Then, with a probability at least $1 - 3e^{-\gamma}$, we have $\mathbf{M} = \mathbf{C}\hat{\mathbf{Z}}$.

Matrix Size Reduction in Stage I of CSMC To ensure a high probability of success, we set $\gamma = \Omega(\ln r)$. Under the standard assumption of a low incoherence parameter $\mu_0(\mathbf{M})$, Theorem 3.2 guarantees exact recovery with $d = \mathcal{O}(r \ln r)$ fully observed columns. Consequently, instead of applying a memory-intensive convex solver to the full $n_1 \times n_2$ matrix, it suffices to complete a much smaller matrix of size $n_1 \times \mathcal{O}(r \ln r)$.

Sample Complexity of Stage II of CSMC While the primary goal of the CSMC method is to provide an efficient two-stage matrix completion procedure, it is important to note that the second stage can also be viewed as a fast standalone matrix completion method under a specific observation model: a subset of d columns of $\mathbf{M} \in \mathbb{R}^{n_1 \times n_2}$ is fully observed, and a subset Ω of entries is observed uniformly at random. Under these assumptions, Theorem 3.2 guarantees exact recovery of \mathbf{M} , requiring $dn_1 + |\Omega|$ observed entries for Stage II. Since $\tilde{r} \leq r$, $\mu_0(\mathbf{C}) \leq \mu_0(\mathbf{M})$, and assuming a small incoherence parameter $\mu_0(\mathbf{M})$, the total number of observed entries simplifies to $\mathcal{O}(r(n_1 + n_2) \ln(n_2 r))$ for $\gamma = \Omega(\ln r)$. By introducing $n = n_1 + n_2$, the sample complexity further simplifies to $\mathcal{O}(rn \ln(nr))$. For comparison, nuclear norm minimization under uniform sampling for matrices with small incoherence parameters, requires $\mathcal{O}(nr \ln^2 n)$ observed entries, while recent modified non-convex gradient descent methods require $\mathcal{O}(r^2 n \ln(n))$ samples [44]. Column sampling approaches like CUR+ [41] achieve $\mathcal{O}(rn \ln(r))$ complexity, and CCS requires $\mathcal{O}(r^2 n \ln^2(n))$ samples [3]. Thus, although the second stage of CSMC does not improve upon the best-known asymptotic sample complexity, it matches leading methods under standard incoherence assumptions and offers significant memory and computational efficiency advantages by solving an ordinary least squares problem.

Choice of sampling columns algorithm To develop a fast and efficient matrix-completion method, we adopt a uniform column sampling strategy, which is computationally inexpensive and does not require access to all matrix entries. Moreover, Xu et al. [41] showed that under the standard incoherence assumption, uniformly sampled columns accurately approximate the column space of a matrix. We acknowledge that uniform sampling does not capture differences between columns. Alternative strategies, such as leverage score sampling [30, 36], volume sampling [45], or determinantal point process sampling [46], may yield better approximations but typically require full access to matrix entries. On the other hand, adaptive sampling methods, while potentially effective for matrices with high incoherence parameters, incur additional computational overhead [37, 39, 40].

3.2 Implementation

The CSMC is a versatile method for solving matrix completion problems. It allows the incorporation of various matrix completion algorithms in the first step and least squares algorithms in the second step. This paper discusses two algorithms that implement the CSMC method, each tailored to address matrix completion problems of different sizes.

1. **Columns Selected Nuclear Norm (CSNN)** in which submatrix is filled with the exact nuclear norm minimization using SDP solver. The CSNN is dedicated to recovering the small and medium size \mathbf{M} . We found the first-order Splitting Conic Solver (SCS) as an efficient way to solve the SDP [47] in the Stage I. To find the optimum of the regression problem (8), we directly solve the least squares for the observed entries in each column. This approach is simple and allows to create fairly efficient distributed implementations.
2. **Columns Selected Proximal Gradient Descent (CSPGD)** in which inexact nuclear norm minimization (4) is solved by Proximal Gradient Descent (PGD). PGD is an efficient first-order method for convex optimization. It leverages the closed formula for the proximal operator for the objective function (4) and allows completing large matrices [15]. To find the optimum of the regression problem (8), we directly solve the least squares for the observed entries in each column.

We have developed and released open-source code implementing both the CSNN minimization algorithm and CSPGD methods. These algorithms support both Numpy arrays [48] and PyTorch tensors [49], with the latter offering the advantage of GPU acceleration for faster computation. The semidefinite programming is solved using the Splitting Conic Solver (SCS) [50]. The code is written in Python 3.10 and is available at <https://github.com/ZAL-NASK/CSMC>.

4 Numerical experiments

All testing examples were implemented in Python 3.10. For benchmarking purposes, the Matrix Factorization (MF) and Iterative SVD algorithms were utilized from the *fancyimpute* library [51].

4.1 Synthetic data set

To evaluate the proposed CSMC method, we compared the performance of the Columns Selected Nuclear Norm algorithm with the exact Nuclear Norm (NN) minimization in a controlled setting. The goal of each experiment was to recover a random 300×1000 matrix \mathbf{M} with the ratio of missing entries ρ . To control the rank of \mathbf{M} equal to r , the test matrix was generated as a product of the $n_1 \times r$ matrix \mathbf{A} and $r \times n_2$ matrix \mathbf{B} . Matrices \mathbf{A} and \mathbf{B} were generated in two steps. In the first one, matrix entries were sampled from the normal distribution $\mathcal{N}(0, 1)$. In the second step, noise matrices with the ratio 0.3 of non-zero entries were added to each matrix.

Experiment S I To assess the sample complexity of the presented methods, we varied the ratio of known entries ρ and the number of sampled columns d . Every setup was executed over $N_{\text{trial}} = 20$ independent trial runs. The performance of the algorithms NN and CSNN- α , $\alpha = \{0.1, \dots, 0.9\}$ was evaluated over all trials. To inquire how many columns should be sampled to achieve a satisfying algorithm relative error,

$$\epsilon := \frac{\|\mathbf{M} - \hat{\mathbf{M}}\|_F}{\|\mathbf{M}\|_F}, \quad (12)$$

we calculated an empirical cumulative distribution function (ECDF) to display the proportion of trials achieved given approximation error [52, 53]. ECDF is defined as $\hat{F}_S : \mathbb{R}_+ \rightarrow [0, 1]$,

$$\hat{F}_S(a) = \frac{|\{s | \epsilon_s \leq a\}|}{|S|}, \quad (13)$$

where each trial is represented as s , ϵ_s denotes the relative error reached by the solution of s , and S denotes the set of all trials for the given parameters setup. We also compared the analyzed algorithms' runtime (in seconds). Since CSMC methods consist of two stages, while other algorithms are one staged, we did not compare iteration numbers of algorithms to achieve solutions of prescribed quality.

Experiment S II With the same experiment settings we benchmarked CSNN- α for $\alpha \in \{0.1, \dots, 0.5\}$ algorithm, Matrix Factorization (MF) [28, 54], Iterative SVD [55], and Nuclear Norm minimization (NN).

Results Experiments were executed on the Linux workstation equipped with 11th Gen Intel(R) Core(TM) i7-1165G7 @ 2.80GHz (8 cores) and 32GB RAM.

Fig. 3 shows that sampling CSNN-0.2 offered a tenfold (10x) increase in time savings compared to the NN algorithm and maintains a solution quality. Although MF was faster than CSNN- α algorithms (Fig. 5), the magnitude of the relative error for CSNN-0.3 and CSNN-0.5 was significantly smaller for rank-5 and rank-10 cases, respectively. In that case, both algorithms returned a solution of superior quality (Fig. 4).

4.2 Recommendation system

Here, we assessed the performance of CSNN and CSPGD algorithms within the context of the Netflix Prize scenario, where matrix completion was employed as a rating prediction technique. Data sets used for the benchmarking are publicly available data sets from the MovieLens research project [56].

Settings To benchmark CSNN and CSPGD algorithms, we constructed two data sets: Movie Lens Small and Movie Lens Big. The Movie Lens Small was represented by $\mathbf{M} \in \mathbb{R}^{140 \times 668}$ matrix obtained from the Movie Lens Small dataset, which contained 100 000 5-star ratings applied to 9742 movies by 610 users. Since the original matrix was too large for SDP solvers, we followed the procedure described in [3] to obtain a submatrix of the desired size. Specifically, we sorted the data by user frequency rate and took data containing rates made by the top 60% users. Then, we sorted the obtained data by movie frequency rate and selected the top 50% movies. The obtained matrix had $\rho = 0.25$ known entries. We evaluate CSPGD algorithms on the MovieLens 25M data set, containing 25 million ratings applied to 62,000 movies by 162,000 users. Again, due to the large size and low observation rate, we extracted a 654×27813 matrix \mathbf{M} . The known entries rate ρ was equal to 0.09.

We assessed the performance of the NN and CSNN- α for $\alpha \in \{0.3, 0.4, 0.5, 0.7\}$ and CSPGD- α for $\alpha \in \{0.3, 0.5\}$. We followed previous work [3] and employed the Cross-Validation method. In each trial of the experiment, Ω set was

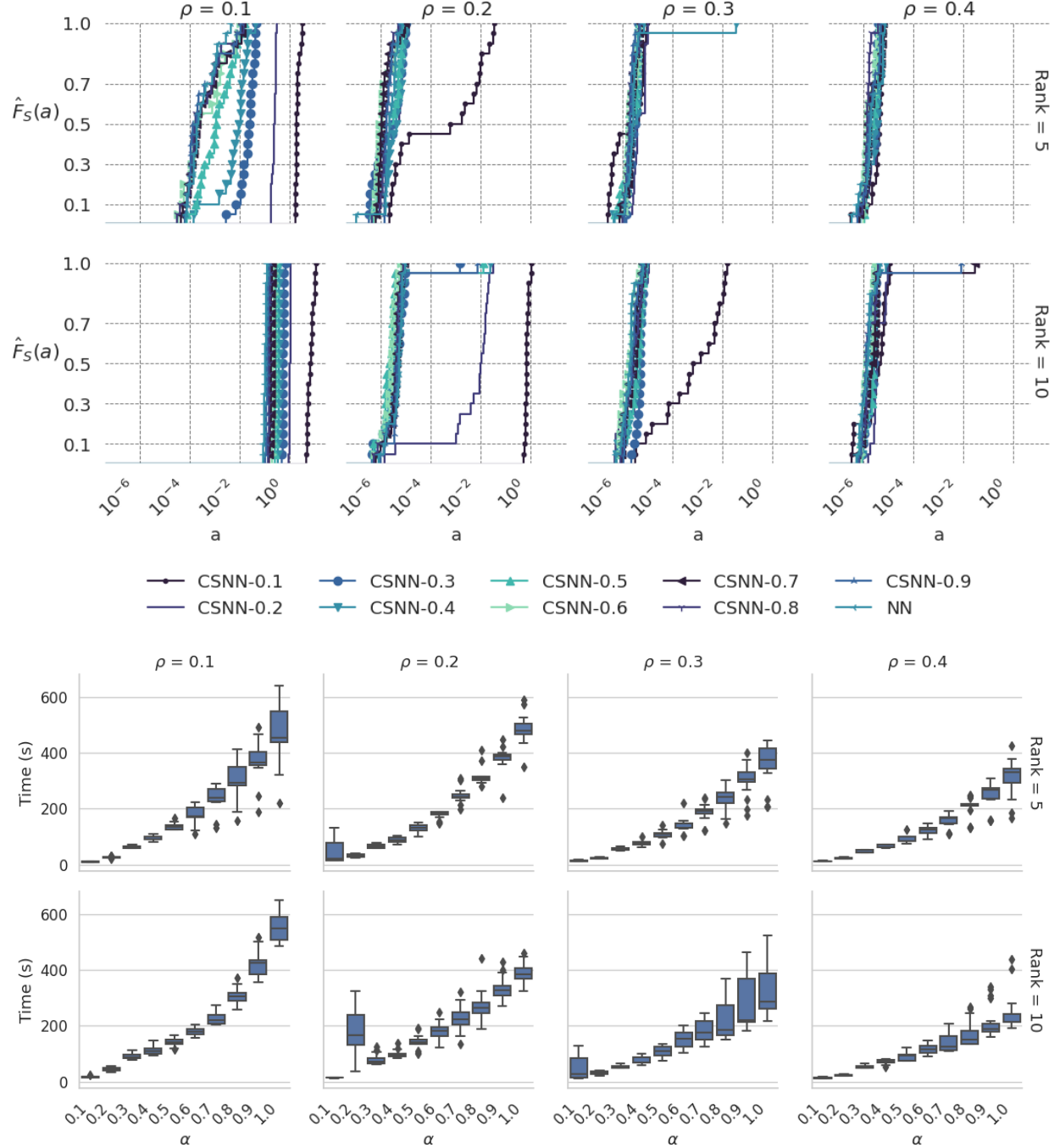


Figure 3: Results S I: ECDF (13) and runtimes depending on the matrix rank and rate of the known entries for NN and CSNN- α , $\alpha \in \{0.1, \dots, 0.9\}$, $M \in \mathbb{R}^{300 \times 1000}$. Sampling with CSNN-0.2 resulted in a tenfold (10x) improvement in time efficiency over the NN algorithm while preserving solution quality.

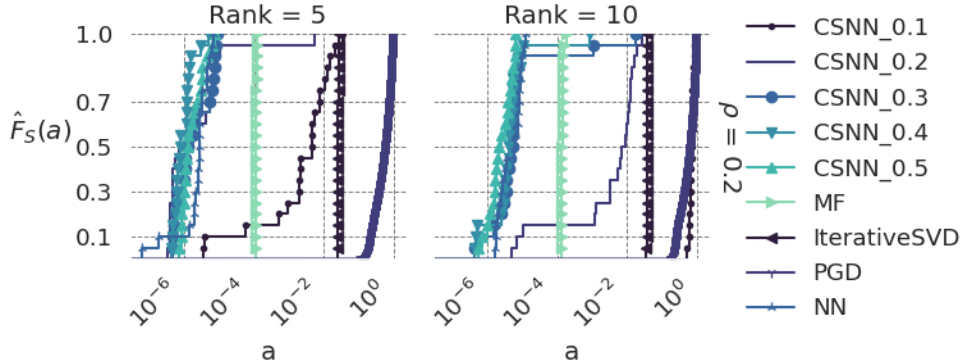


Figure 4: Results S II: ECDF (13) curves depending on the matrix rank and rate of the known entries for NN and CSNN- α , $\alpha \in \{0.1, \dots, 0.9\}$, $\mathbf{M} \in \mathbb{R}^{300 \times 1000}$. The relative error magnitude for CSNN-0.3 and CSNN-0.5 was notably lower in rank-5 and rank-10 scenarios, respectively, compared to MF.

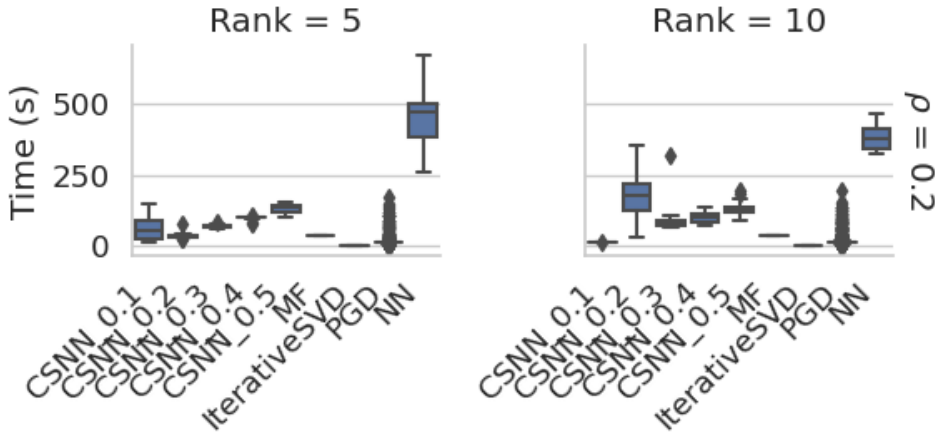


Figure 5: Results S II: ECDF (13) curves depending on the matrix rank and rate of the known entries for NN and CSNN- α , $\alpha \in \{0.1, \dots, 0.9\}$, $\mathbf{M} \in \mathbb{R}^{300 \times 1000}$.

randomly split into training and testing sets denoted by Ω_{train} and Ω_{test} [57]. Specifically, we randomly selected ρ rate of the observed set, and by assigning the null values to the rest of the entries, we constructed $\mathcal{R}_{\Omega_{\text{train}}}(\mathbf{M})$ matrix. We evaluated each algorithm on the Ω_{test} set. We conducted 20 independent experimental trials under each scenario.

We compared Normalized Mean Absolute Error (NMAE) calculated as

$$\text{NMAE} = \frac{1}{|\Omega_{\text{test}}|(m_{\max} - m_{\min})} \sum_{(i,j) \in \Omega_{\text{test}}} |\hat{m}_{ij} - m_{ij}|, \quad (14)$$

where m_{\max} and m_{\min} denote the maximum and minimum rating, respectively, and Ω_{test} denotes the set of indices in test set. This metric is widely used to assess collaborative filtering tasks [3]. The quality of the recommendation was also measured as hit-rate, defined as

$$\text{HR} = \frac{\#\text{hits}}{|\Omega_{\text{test}}|}, \quad (15)$$

where a predicted rating was considered a *hit* if its rounded value equals the actual rating in the test set [3].

Results Fig. 6 shows that the predictions of CSNN-0.7 maintained the quality of the NN algorithm in terms of NMAE: (0.16 vs 0.13) and HR (0.23 vs 0.25), and results in runtime savings from 57 seconds to 40 seconds (Table 2). CSPGD

Algorithm	NMAE		HR		Time [s]	
	mean	std	mean	std	mean	std
CSNN-0.3	0.271	0.028	0.172	0.005	10.137	1.118
CSNN-0.4	0.240	0.060	0.191	0.005	17.677	2.005
CSNN-0.5	0.248	0.176	0.208	0.006	28.673	2.419
CSNN-0.7	0.156	0.011	0.232	0.004	39.893	8.595
NN	0.127	0.001	0.255	0.006	56.924	2.435

Table 2: Results on Movie Lens Small dataset; NN and CSNN- α algorithms, $\alpha \in \{0.3, 0.4, 0.5, 0.7\}$.

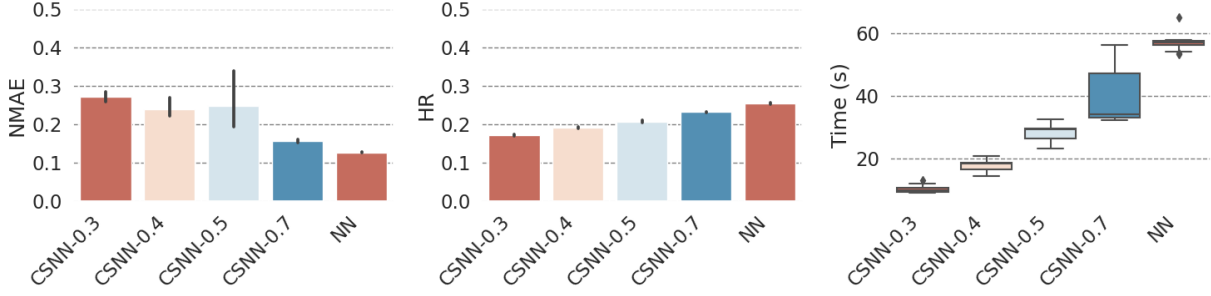


Figure 6: Results on Movie Lens Small dataset; NN and CSNN- α algorithms, $\alpha \in \{0.3, 0.4, 0.5, 0.7\}$.

algorithms were much faster than PGD (Fig. 7). The HR values for PGD and CSPGD-0.3 were equal to 0.28 and 0.24, respectively (Table 3).

4.3 Image recovery

Image inpainting, a technique in image processing and computer vision, fills in missing or corrupted parts. Additionally, estimating random missing pixels can be treated as a denoising method or utilized to accelerate rendering processes. Low-rank models are highly effective for this task, leveraging the assumption that images typically exhibit low-rank structures. The primary information of the image matrix is dominated by its largest singular values while setting the smallest singular values to zero can be done without losing essential details.

Settings The data set contained ten grey-scaled pictures of bridges downloaded from the public repository¹. Images were represented as 240×360 matrices. We assessed the performance of the algorithms among 100 independent trials (ten trials per picture). The quality of the reconstructed image was assessed with the signal-to-noise ratio (SNR)

$$\text{SNR}(\hat{\mathbf{M}}) = 20 \log_{10} \left(\frac{\|\mathbf{M}\|_F}{\|\hat{\mathbf{M}} - \mathbf{M}\|_F} \right) \quad (16)$$

and the relative error (12).

¹image source (<https://pxhere.com/p1/>)

Algorithm	NMAE		HR		Time [s]	
	mean	std	mean	std	mean	std
CSPGD-0.3	0.138	0.001	0.245	0.002	23.032	0.321
CSPGD-0.5	0.135	0.001	0.252	0.001	27.774	0.299
PGD	0.119	0.001	0.281	0.001	449.026	9.502

Table 3: Results on Movie Lens Big dataset; PGD and CSPGD- α algorithms for $\alpha \in \{0.3, 0.5\}$.

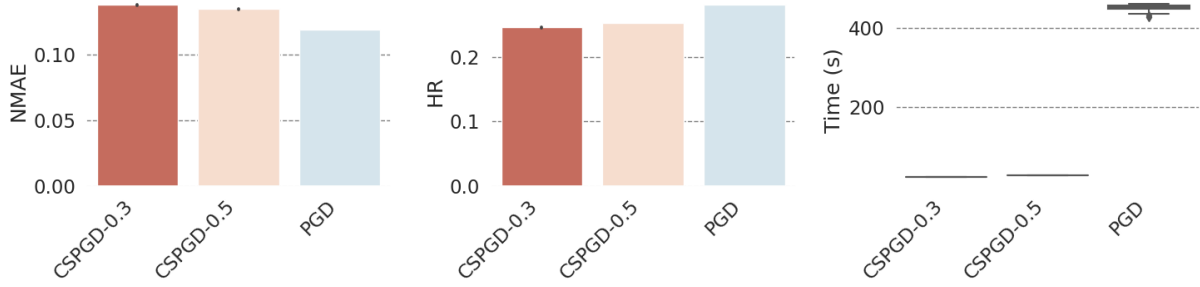


Figure 7: Results on Movie Lens Big dataset; PGD and CSPGD- α algorithms for $\alpha \in \{0.3, 0.5\}$.



Bridge restored with NN. Bridge restored with CSNN-0.7
Figure 8: Image inpainting; NN and CSNN-0.7 algorithms, $\rho = 20\%$ known entries.

Results The CSNN-0.7 solutions maintained the quality of the NN in terms of SNR (Table 4). As shown in Fig. 9, CSNN-0.5 offered considerable time savings and good relative error. Fig. 8 presents one of the completed pictures.

5 Conclusion

This paper introduces the Columns Selected Matrix Completion (CSMC) method, which enhances the time efficiency of nuclear norm minimization algorithms for low-rank matrix completion. CSMC employs a two-stage approach: first, it applies a low-rank matrix completion algorithm to a reduced problem size, followed by minimizing the least squares error. Theoretical analysis provides provable guarantees for perfect matrix recovery under standard assumptions.

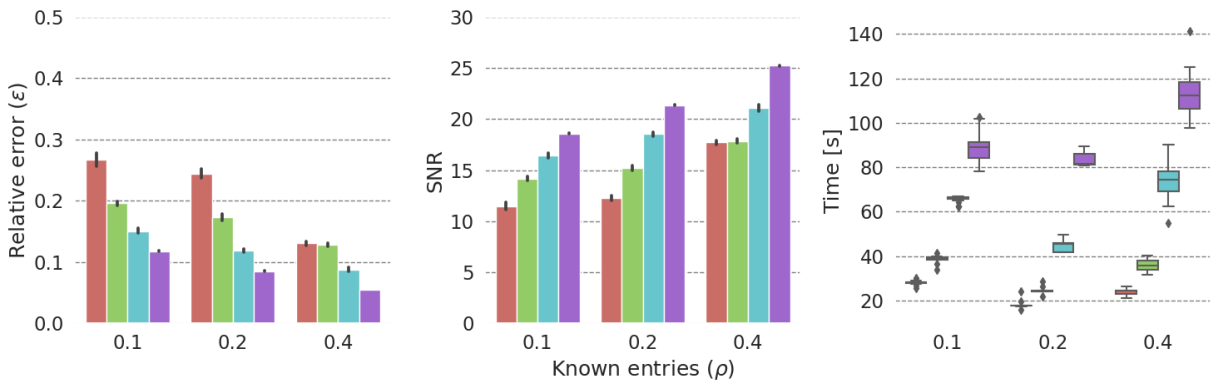


Figure 9: Results for image inpainting; NN and CSNN- α algorithms for $\alpha \in \{0.3, 0.4, 0.5, 0.7\}$.

Known entries ratio ρ Algorithm	SNR			Relative error (ϵ)			Time [s]		
	0.4	0.2	0.1	0.4	0.2	0.1	0.4	0.2	0.1
CSNN_0.3	18.844	10.829	7.366	0.114	0.289	0.438	16.306	12.026	19.365
CSNN_0.4	17.708	12.245	11.491	0.130	0.245	0.268	24.151	17.997	28.123
CSNN_0.5	17.851	15.245	14.172	0.128	0.173	0.196	35.719	24.424	38.647
CSNN_0.7	21.134	18.526	16.458	0.088	0.119	0.151	73.670	44.948	65.639
NN	25.221	21.377	18.582	0.055	0.085	0.118	113.215	83.196	88.966

Table 4: Results for image inpainting; NN and CSNN- α , $\alpha \in \{0.3, 0.4, 0.5, 0.7\}$.

Numerical simulations show that CSMC significantly reduces computational time while maintaining high accuracy in the reconstructed data. Compared to alternative methods, CSMC demonstrates competitive performance in approximating missing entries. This enhanced time efficiency is particularly valuable for tasks such as recommendation systems, image processing, and other matrix-based applications, where large, incomplete datasets must be effectively recovered. Reducing computational time while minimizing accuracy loss is crucial for enabling efficient processing of incomplete data, which is central to many real-world applications in pattern recognition.

CSMC relies on uniform column sampling and nuclear norm-based algorithms, but its flexible framework allows for the integration of alternative sampling strategies and matrix completion techniques. Future work will explore adaptive sampling approaches, such as those proposed in recent studies [37, 39], to handle high-coherence matrices and reduce sample complexity.

Acknowledgments

The authors thank Dr. Aikaterini Aretaki for her critical review and comments on the manuscript.

Appendix A Proof of Theorem 3.2 and supporting theorems

We present a comprehensive proof of Theorem 3.2, accompanied by the development of two additional theorems, namely A.2 and A.4, which are our original contributions. The proofs for these supplementary theorems are provided within this work. Additionally, the cited theorems from the literature have their proofs outlined therein.

We assume that $\mathbf{C} \in \mathbb{R}^{n_1 \times d}$ is a column submatrix of $\mathbf{M} \in \mathbb{R}^{n_1 \times n_2}$. \mathbf{C} is obtained by sampling uniformly without replacement d columns of \mathbf{M} . Let r be the rank of \mathbf{M} and let \tilde{r} be the rank of \mathbf{C} . We assume that the compact SVD of \mathbf{C} is given by,

$$\mathbf{C} = \tilde{\mathbf{U}} \tilde{\Sigma} \tilde{\mathbf{V}}^T, \quad (17)$$

where $\tilde{\mathbf{U}} \in \mathbb{R}^{n_1 \times \tilde{r}}$, $\tilde{\mathbf{V}} \in \mathbb{R}^{n_2 \times \tilde{r}}$, and $\tilde{\Sigma} \in \mathbb{R}^{\tilde{r} \times \tilde{r}}$.

We denote as $\mu_0(\mathbf{M})$ and $\mu_0(\mathbf{C})$ the coherence parameters of \mathbf{M} and \mathbf{C} .

We denote as \tilde{U} the subspace spanned by the first \tilde{r} left singular vectors of \mathbf{C} . The orthogonal projection onto \tilde{U} is given by

$$P_{\tilde{U}} = \tilde{\mathbf{U}} \tilde{\mathbf{U}}^T. \quad (18)$$

The following lemma can be found in [41] and shows that under the incoherence assumption, uniform sampling outputs a high-quality solution to the CSS problem, with high quality.

Theorem A.1 (Theorem 9 in Xu et al. [41]). *Let \tilde{U}_ψ denote subspace spanned by the ψ first left singular vectors of \mathbf{C} and let $P_{\tilde{U}_\psi}$ denote orthogonal projection onto \tilde{U}_ψ . Then for parameter $\gamma > 0$, with probability $1 - 2e^{-\gamma}$ we have*

$$\|\mathbf{M} - P_{\tilde{U}_\psi} \mathbf{M}\|_2^2 \leq \sigma_{\psi+1}^2 \left(1 + \frac{2n_2}{d}\right), \quad (19)$$

if $d \geq 7\mu(U_\psi)\psi(\gamma + \ln \psi)$, where d denotes number of sampled columns in \mathbf{C} , $\sigma_{\psi+1}$ is the $(\psi + 1)$ -th largest singular value of \mathbf{M} and $\mu(U_\psi)$ is the coherence of the subspace spanned by ψ first left singular vectors of \mathbf{M} ,

The following remark is the immediate consequence of the Theorem A.1.

Remark A.1. Let $\psi \geq r$, where r is the rank of \mathbf{M} . Then $\sigma_{\psi+1} = \sigma_{r+1} = 0$ and with probability $1 - 2e^{-\gamma}$,

$$\|\mathbf{M} - P_{\tilde{U}}\mathbf{M}\|_2^2 = 0, \quad (20)$$

provided that $d \geq 7\mu_0(\mathbf{M})r(\gamma + \ln r)$.

We now bound the distance measured in the spectral norm between \mathbf{M} and $\hat{\mathbf{M}} = \mathbf{C}\hat{\mathbf{Z}}$. To do that, we assume that the objective function $g : \mathbb{R}^{\tilde{r} \times n_2} \rightarrow \mathbb{R}$,

$$g(\mathbf{Y}) = \frac{1}{2}\|\mathcal{R}_\Omega(\mathbf{M}) - \mathcal{R}_\Omega(\tilde{\mathbf{U}}\mathbf{Y})\|_F^2 \quad (21)$$

is strongly convex [58], where the strong convexity is defined as follows.

Definition A.1 (Boyd and Vandenberghe [58]). A function $g : \mathbb{R}^{\tilde{r} \times n_2} \rightarrow \mathbb{R}$ is strongly convex with parameter $\beta > 0$ if $h(\mathbf{X}) = g(\mathbf{X}) - \frac{\beta}{2}\|\mathbf{X}\|_F^2$ is convex.

The following remarks provide a helpful characterization of strongly convex functions.

Remark A.2 (Boyd and Vandenberghe [58]). A function $g : \mathbb{R}^{\tilde{r} \times n_2} \rightarrow \mathbb{R}$ is strongly convex with parameter $\beta > 0$ if g is everywhere differentiable and

$$g(\mathbf{Y}) \geq g(\mathbf{X}) + \langle \nabla g(\mathbf{X}), \mathbf{Y} - \mathbf{X} \rangle + \frac{\beta}{2}\|\mathbf{Y} - \mathbf{X}\|_F^2, \quad (22)$$

for any $\mathbf{X}, \mathbf{Y} \in \mathbb{R}^{\tilde{r} \times n_2}$, where inner product is defined as

$$\langle \mathbf{X}, \mathbf{Y} \rangle = \text{tr}(\mathbf{X}^T \mathbf{Y}). \quad (23)$$

Remark A.3 (Boyd and Vandenberghe [58]). If g is twice differentiable, then $g(\mathbf{X})$ is strongly convex with parameter $\beta > 0$ if $\nabla^2 g(\mathbf{X}) \succeq \beta \mathbf{I}$ for any $\mathbf{X} \in \mathbb{R}^{\tilde{r} \times n_2}$.

We now provide the formula for the first-order and the second-order partial derivatives of g . Let y_{sw} denote the (s, w) entry of the matrix \mathbf{Y} , and m_{lw} denote (l, w) entry of \mathbf{M} then the partial derivative of g with respect to y_{sw} is given by following formula,

$$\frac{\partial g}{\partial y_{sw}} = - \sum_{l:(l,w) \in \Omega} (m_{lw} - \sum_{i=1}^{\tilde{r}} \tilde{u}_{li} y_{iw}) \tilde{u}_{ls} = \sum_{l:(l,w) \in \Omega} (\sum_{i=1}^{\tilde{r}} \tilde{u}_{li} y_{iw} - m_{lw}) \tilde{u}_{ls}. \quad (24)$$

The second-order partial derivative with respect to y_{pq} and y_{sw} is equal to

$$\frac{\partial^2 g}{\partial y_{sw} \partial y_{pq}} = \begin{cases} \sum_{l:(l,w) \in \Omega} \tilde{u}_{ls} \tilde{u}_{lp} & w = q, \\ 0 & w \neq q. \end{cases} \quad (25)$$

The following theorem shows that under certain assumptions, $\hat{\mathbf{M}} = \mathbf{C}\hat{\mathbf{Z}}$ is close to the matrix \mathbf{M} in the spectral norm. Those assumptions include that i) $P_{\tilde{U}}\mathbf{M}$ is close to \mathbf{M} , ii) g is strongly convex with parameter β . The following proofs take inspiration from the work of Xu et al. [41].

Theorem A.2. Suppose that $\|\mathbf{M} - P_{\tilde{U}}\mathbf{M}\|_2^2 \leq \Delta$ for the parameter $\Delta > 0$, and let \tilde{U} be the subspace of \mathbb{R}^{n_1} spanned by the first \tilde{r} left singular vectors of \mathbf{C} , $P_{\tilde{U}} = \tilde{\mathbf{U}}\tilde{\mathbf{U}}^T$. Assume that g is strongly convex with a parameter β , then

$$\|\mathbf{M} - \hat{\mathbf{M}}\|_2^2 \leq 2\Delta + \frac{4n_1\Delta}{\beta}. \quad (26)$$

Proof. Set $\mathbf{Y}_1 = \tilde{\mathbf{U}}^T \mathbf{M}$, then from the assumptions

$$\|\mathbf{M} - \tilde{\mathbf{U}}\mathbf{Y}_1\|_2^2 \leq \Delta. \quad (27)$$

Thus

$$\frac{1}{r'} \|\mathbf{M} - \tilde{\mathbf{U}}\mathbf{Y}_1\|_F^2 \leq \|\mathbf{M} - \tilde{\mathbf{U}}\mathbf{Y}_1\|_2^2 \leq \Delta, \quad (28)$$

where r' denotes the rank of the matrix $(\mathbf{M} - \tilde{\mathbf{U}}\mathbf{Y}_1) \in \mathbb{R}^{n_1 \times n_2}$ and

$$\|\mathcal{R}_\Omega(\mathbf{M}) - \mathcal{R}_\Omega(\tilde{\mathbf{U}}\mathbf{Y}_1)\|_F^2 \leq \|\mathbf{M} - \tilde{\mathbf{U}}\mathbf{Y}_1\|_2^2 \leq r'\Delta. \quad (29)$$

Since any of the matrix dimensions bounds rank, $r' \leq n_1$ (for thick matrices $n_1 < n_2$)

$$\|\mathcal{R}_\Omega(\mathbf{M}) - \mathcal{R}_\Omega(\tilde{\mathbf{U}}\mathbf{Y}_1)\|_F^2 \leq n_1\Delta. \quad (30)$$

Let $\hat{\mathbf{Z}}$ be a solution to the problem 11, then

$$f(\hat{\mathbf{Z}}) = \|\mathcal{R}_\Omega(\mathbf{M}) - \mathcal{R}_\Omega(\mathbf{C}\hat{\mathbf{Z}})\|_F^2 = \|\mathcal{R}_\Omega(\mathbf{M}) - \mathcal{R}_\Omega(\tilde{\mathbf{U}}\tilde{\Sigma}\tilde{\mathbf{V}}^T\hat{\mathbf{Z}})\|_F^2 \quad (31)$$

and $\hat{\mathbf{Y}} := \tilde{\Sigma}\tilde{\mathbf{V}}^T\hat{\mathbf{Z}}$ must be a minimum of g . Indeed, assume that $g(\mathbf{Y}_2) < g(\hat{\mathbf{Y}})$ for some $\mathbf{Y}_2 \neq \hat{\mathbf{Y}}$, i.e.

$$\begin{aligned} \|\mathcal{R}_\Omega(\mathbf{M}) - \mathcal{R}_\Omega(\mathbf{C}\hat{\mathbf{Z}})\|_F^2 &= \|\mathcal{R}_\Omega(\mathbf{M}) - \mathcal{R}_\Omega(\tilde{\mathbf{U}}\hat{\mathbf{Y}})\|_F^2 \\ &> \|\mathcal{R}_\Omega(\mathbf{M}) - \mathcal{R}_\Omega(\tilde{\mathbf{U}}\mathbf{Y}_2)\|_F^2 \\ &= \|\mathcal{R}_\Omega(\mathbf{M}) - \mathcal{R}_\Omega(\mathbf{C}\underbrace{\tilde{\mathbf{V}}\tilde{\Sigma}^{-1}\mathbf{Y}_2}_{\mathbf{X}_2})\|_F^2 \end{aligned} \quad (32)$$

and $f(\mathbf{X}_2) < f(\hat{\mathbf{Z}})$ where f is the objective function in problem 11.

We bound distance between \mathbf{Y}_1 and $\hat{\mathbf{Y}}$ using strong convexity of g . Since $\hat{\mathbf{Y}}$ is minimum of $g(\mathbf{Y})$ (21), then $\nabla g(\hat{\mathbf{Y}}) = \mathbf{0}$, and

$$\langle \nabla g(\hat{\mathbf{Y}}), \mathbf{Y}_1 - \hat{\mathbf{Y}} \rangle = 0. \quad (33)$$

Thus, by the Remark A.2,

$$g(\mathbf{Y}_1) \geq g(\hat{\mathbf{Y}}) + \frac{\beta}{2} \|\mathbf{Y}_1 - \hat{\mathbf{Y}}\|_F^2. \quad (34)$$

Using the definition of g given in (21),

$$\begin{aligned} \frac{\beta}{2} \|\mathbf{Y}_1 - \hat{\mathbf{Y}}\|_F^2 &\leq \|\mathcal{R}_\Omega(\mathbf{M}) - \mathcal{R}_\Omega(\tilde{\mathbf{U}}\mathbf{Y}_1)\|_F^2 - \|\mathcal{R}_\Omega(\mathbf{M}) - \mathcal{R}_\Omega(\tilde{\mathbf{U}}\hat{\mathbf{Y}})\|_F^2 \\ &\leq \|\mathcal{R}_\Omega(\mathbf{M}) - \mathcal{R}_\Omega(\tilde{\mathbf{U}}\mathbf{Y}_1)\|_F^2. \end{aligned} \quad (35)$$

Combining (35) and (30),

$$\|\mathbf{Y}_1 - \hat{\mathbf{Y}}\|_F^2 \leq \frac{2}{\beta} \|\mathcal{R}_\Omega(\mathbf{M}) - \mathcal{R}_\Omega(\tilde{\mathbf{U}}\mathbf{Y}_1)\|_F^2 \leq \frac{2n_1}{\beta} \Delta. \quad (36)$$

By applying the triangle inequality, Cauchy-Schwarz inequality, and leveraging the fact that the Frobenius norm is an upper bound for the spectral norm,

$$\begin{aligned}\|\mathbf{M} - \hat{\mathbf{M}}\|_2^2 &= \|\mathbf{M} - \mathbf{C}\hat{\mathbf{Z}}\|_2^2 \\ &\leq 2\|\mathbf{M} - \tilde{\mathbf{U}}\tilde{\mathbf{U}}^T\mathbf{M}\|_2^2 + 2\|\tilde{\mathbf{U}}\tilde{\mathbf{U}}^T\mathbf{M} - \mathbf{C}\hat{\mathbf{Z}}\|_2^2 \\ &\leq 2\|\mathbf{M} - P_{\tilde{\mathbf{U}}}\mathbf{M}\|_2^2 + 2\|\tilde{\mathbf{U}}\tilde{\mathbf{U}}^T\mathbf{M} - \mathbf{C}\hat{\mathbf{Z}}\|_F^2.\end{aligned}\tag{37}$$

The first component on the right side is bounded by the assumptions,

$$\|\mathbf{M} - P_{\tilde{\mathbf{U}}}\mathbf{M}\|_2^2 \leq \Delta.\tag{38}$$

To bound the second component, we use the definition of the \mathbf{Y}_1 and $\hat{\mathbf{Y}}$,

$$\|\tilde{\mathbf{U}}\tilde{\mathbf{U}}^T\mathbf{M} - \tilde{\mathbf{U}}\tilde{\Sigma}\tilde{\mathbf{V}}^T\hat{\mathbf{Z}}\|_F^2 = \|\tilde{\mathbf{U}}(\mathbf{Y}_1 - \hat{\mathbf{Y}})\|_F^2 \leq \|\tilde{\mathbf{U}}\|_2^2\|\mathbf{Y}_1 - \hat{\mathbf{Y}}\|_F^2 = \|\mathbf{Y}_1 - \hat{\mathbf{Y}}\|_F^2.\tag{39}$$

Using (36), we obtain the following bound:

$$\|\mathbf{M} - \hat{\mathbf{M}}\|_2^2 \leq 2\Delta + \frac{4n_1\Delta}{\beta}.\tag{40}$$

□

To bound the parameter β of the strong convexity, we use Remark A.3 and bound the smallest eigenvalue of the Hessian of g . Following [41], to do that, we use the following result of Tropp [59].

Theorem A.3 (Theorem 5 in Xu et al. [41] derived from Theorem 2.2 in Tropp [59]). *Let \mathcal{X} be a finite set of the positive-semidefinite (PSD) matrices with dimension $k \times k$, and suppose that*

$$\max_{\mathbf{X} \in \mathcal{X}} \lambda_{\max}(\mathbf{X}) \leq B\tag{41}$$

for some parameter $B > 0$, where $\lambda_{\max}(\mathbf{X})$ is the maximum eigenvalue of \mathbf{X} . Sample $\{\mathbf{X}_1, \dots, \mathbf{X}_\Psi\}$ uniformly at random from \mathcal{X} without replacement. Compute:

$$\mu_{\min} := \Psi \lambda_{\min}(\mathbb{E}\mathbf{X}_1),\tag{42}$$

and

$$\mu_{\max} := \Psi \lambda_{\max}(\mathbb{E}\mathbf{X}_1),\tag{43}$$

where $\mathbb{E}\mathbf{X}_1$ is the expected value of a random variable \mathbf{X}_1 , $\lambda_{\max}(\mathbb{E}\mathbf{X}_1)$ and $\lambda_{\min}(\mathbb{E}\mathbf{X}_1)$ denote its maximum and minimum eigenvalue.

$$P\left(\lambda_{\max}\left(\sum_{j=1}^{\Psi} \mathbf{X}_j\right) \geq (1+\rho)\mu_{\max}\right) \leq k \exp \frac{-\mu_{\max}}{B}[(1+\rho) \ln (1+\rho) - \rho],\tag{44}$$

for parameter $\rho \in [0, 1)$.

$$P\left(\lambda_{\min}\left(\sum_{j=1}^{\Psi} \mathbf{X}_j\right) \leq (1-\rho)\mu_{\min}\right) \leq k \exp \frac{-\mu_{\min}}{B}[(1-\rho) \ln (1-\rho) + \rho],\tag{45}$$

for parameter $\rho \geq 0$.

Theorem A.4. Let $\gamma > 0$ be a parameter. With probability $1 - e^{-\gamma}$ we have that the objective function $g : \mathbb{R}^{\tilde{r} \times n_2} \rightarrow \mathbb{R}$ defined in (21) is strongly convex with parameter $\beta > 0$, provided that

$$|\Omega| \geq \tilde{r}n_2\mu(\tilde{U}) \left(\gamma + \ln \left(\frac{n_2\tilde{r}}{2} \right) \right). \quad (46)$$

Proof. By remark A.3 to bound strong convexity, we can instead bound the smallest eigenvalue of the Hessian matrix $\mathbf{H} = \nabla^2 g$.

The Hessian matrix of a function g is a $\tilde{r}n_2 \times \tilde{r}n_2$ matrix. Let us assume that second-order derivative with respect to the y_{sw} and y_{pq} entries of matrix \mathbf{Y} is the $(\tilde{r}(s-1) + w, \tilde{r}(p-1) + q)$ entry of the Hessian matrix. Then using eq. 25 the Hessian matrix \mathbf{H} can be written as

$$\begin{pmatrix} \mathbf{H}^{1,1} & \mathbf{H}^{1,2} & \dots & \mathbf{H}^{1,\tilde{r}} \\ \mathbf{H}^{2,1} & \ddots & \dots & \mathbf{H}^{2,\tilde{r}} \\ \vdots & \vdots & \ddots & \vdots \\ \mathbf{H}^{\tilde{r},1} & \mathbf{H}^{\tilde{r},2} & \dots & \mathbf{H}^{\tilde{r},\tilde{r}} \end{pmatrix} \quad (47)$$

where $\mathbf{H}^{s,q}$ is a diagonal $n_2 \times n_2$ matrix containing partial derivatives $\frac{\partial^2 g}{\partial y_{sw} \partial y_{pq}}$ for $w, q \in \{1, \dots, n_2\}$.

$$\mathbf{H}^{s,q} = \begin{pmatrix} \sum_{l:(l,1) \in \Omega} \tilde{u}_{ls} \tilde{u}_{lp} & 0 & \dots & 0 \\ 0 & \ddots & \dots & 0 \\ \vdots & \vdots & \ddots & \vdots \\ 0 & 0 & \dots & \sum_{l:(l,n_2) \in \Omega} \tilde{u}_{ls} \tilde{u}_{lp} \end{pmatrix} \quad (48)$$

Then the Hessian of g is a sum of the random matrices,

$$\mathbf{H} = \sum_{(i,j) \in \Omega} \tilde{\mathbf{u}}_{i:} \tilde{\mathbf{u}}_{i:}^T \otimes \mathbf{e}_j \mathbf{e}_j^T, \quad (49)$$

where $\mathbf{e}_j \in \mathbb{R}^{n_2}$ is a standard basis vector and $\tilde{\mathbf{u}}_{i:} \in \mathbb{R}^r$ is a vector defined by the i -th row of matrix $\tilde{\mathbf{U}}$, and \otimes denote the Kronecker product.

Thus the Hessian of g is a sum of the $|\Omega|$ random matrices of the form

$$\mathbf{H}^{i,j} := \tilde{\mathbf{u}}_{i:} \tilde{\mathbf{u}}_{i:}^T \otimes \mathbf{e}_j \mathbf{e}_j^T, \quad (50)$$

where $\tilde{\mathbf{u}}_{i:} \tilde{\mathbf{u}}_{i:}^T \in \mathbb{R}^{\tilde{r} \times \tilde{r}}$ is PSD and $\mathbf{e}_j \mathbf{e}_j^T \in \mathbb{R}^{n_2 \times n_2}$ is also PSD. Thus,

$$\mathbf{H} = \sum_{(i,j) \in \Omega} \mathbf{H}^{i,j}. \quad (51)$$

Each $\mathbf{H}^{i,j}$ is PSD as the Kronecker product of the two PSD matrices. Moreover,

$$\lambda_{\max}(\mathbf{H}^{i,j}) = \lambda_{\max}(\tilde{\mathbf{u}}_{i:} \tilde{\mathbf{u}}_{i:}^T) = \sum_{j=1}^{\tilde{r}} \tilde{u}_{ij}^2 = \|\tilde{\mathbf{u}}_{i:}\|_2^2 \leq \frac{\tilde{r}\mu(\tilde{U})}{n_1} \quad (52)$$

for each $i = 1, \dots, n_1, j = 1, \dots, n_2$.

Let (i_1, j_1) be the first pair of indices in Ω , i.e., the indices of the first observed entry in \mathbf{M} . The expected value of the random matrix \mathbf{H}^{i_1, j_1} is given by

$$\begin{aligned}
\mathbb{E}(\mathbf{H}^{i_1, j_1}) &= \frac{1}{n_1 n_2} \sum_{l=1}^{n_1} \sum_{q=1}^{n_2} \mathbf{H}^{l,q} \\
&= \frac{1}{n_1 n_2} \tilde{\mathbf{U}}^T \tilde{\mathbf{U}} \otimes \mathbf{I}_{n_1 \times n_1} \\
&= \frac{1}{n_1 n_2} \mathbf{I}_{\tilde{r} \times \tilde{r}} \otimes \mathbf{I}_{n_1 \times n_1} \\
&= \frac{1}{n_1 n_2} \mathbf{I}_{\tilde{r} n_1 \times \tilde{r} n_1}.
\end{aligned} \tag{53}$$

Following the notation of Theorem A.3,

$$\mu_{\min} = |\Omega| \lambda_{\min}(\mathbb{E}(\mathbf{H}^{i_1, j_1})) = \frac{|\Omega|}{n_1 n_2}, \tag{54}$$

and

$$\max_{ij} \lambda_{\max}(\mathbf{H}^{i,j}) \leq \frac{\tilde{r} \mu(\tilde{U})}{n_1} = B. \tag{55}$$

Combining Theorem A.3 with $\rho = \frac{1}{2}$ and eq. (51)

$$P(\lambda_{\min}(\mathbf{H}) \leq \frac{1}{2} \mu_{\min}) \leq \tilde{r} n_2 \exp\left(\frac{-\mu_{\min}}{B}\right) \left(\frac{1 - \ln 2}{2}\right) \leq \frac{\tilde{r} n_2}{2} \exp\left(\frac{-\mu_{\min}}{B}\right), \tag{56}$$

implying,

$$P\left(\lambda_{\min}(\mathbf{H}) \leq \frac{|\Omega|}{2 n_1 n_2}\right) \leq \frac{\tilde{r} n_2}{2} \exp\left(-\frac{|\Omega|}{\tilde{r} n_2 \mu(\tilde{U})}\right), \tag{57}$$

Hence, with probability at least $1 - e^{-\gamma}$,

$$\lambda_{\min}(\mathbf{H}) \geq \frac{|\Omega|}{2 n_1 n_2}, \tag{58}$$

provided that

$$|\Omega| \geq \tilde{r} n_2 \mu(\tilde{U}) \left(\gamma + \ln\left(\frac{n_2 \tilde{r}}{2}\right)\right). \tag{59}$$

□

Theorem 3.2 can be proved by combining the results of Theorems A.2 and A.4.

Proof of Theorem 3.2.

Since $d \geq 7\mu_0(\mathbf{M})r(\gamma + \ln r)$, from the Remark A.1, we have

$$\|\mathbf{M} - P_{\tilde{U}} \mathbf{M}\|_2^2 = 0, \tag{60}$$

with the probability at least $1 - 2e^{-\gamma}$.

From Theorem A.4, the fact that $\mu_0(\mathbf{C}) > \mu(\tilde{U})$ and the fact $|\Omega| \geq \tilde{r}n_2\mu_0(\mathbf{C})\left(\gamma + \ln\left(\frac{n_2\tilde{r}}{2}\right)\right)$, function g is β -strongly convex with probability at least $1 - e^{-\gamma}$.

The probability the fact, that eq. (60) holds and g is β -strongly convex is grater or equal than $(1 - 3e^{-\gamma}) + (1 - e^{-\gamma}) - 1$.

Thus we can apply Theorem A.2 with $\Delta = 0$ and show that

$$\|\mathbf{M} - \hat{\mathbf{M}}\|_2^2 \leq 0, \quad (61)$$

implying $\mathbf{M} = \hat{\mathbf{M}}$ with probability at least $1 - 3e^{-\gamma}$.

□

References

- [1] Tianxi Cai, T. Cai, and Anru Zhang. Structured matrix completion with applications to genomic data integration. *Journal of the American Statistical Association*, 111, 04 2015.
- [2] Hanqin Cai, Jian-Feng Cai, and Juntao You. Structured gradient descent for fast robust low-rank hankel matrix completion. *SIAM Journal on Scientific Computing*, 45(3):A1172–A1198, 2023.
- [3] HanQin Cai, Longxiu Huang, Pengyu Li, and Deanna Needell. Matrix completion with cross-concentrated sampling: Bridging uniform sampling and cur sampling. *IEEE Transactions on Pattern Analysis and Machine Intelligence*, 2023.
- [4] Mikael Le Pendu, Xiaoran Jiang, and Christine Guillemot. Light field inpainting propagation via low rank matrix completion. *IEEE Transactions on Image Processing*, 27(4):1981–1993, 2018.
- [5] Ankur Moitra. *Algorithmic Aspects of Machine Learning*. Cambridge University Press, USA, 1st edition, 2018.
- [6] Hongyuan Zhang, Ziheng Jiao, and Xuelong Li. Orthogonal subspace exploration for matrix completion. *Pattern Recognition*, 153:110456, 2024.
- [7] Ziheng Li, Feiping Nie, Rong Wang, and Xuelong Li. Robust rank-one matrix completion with rank estimation. *Pattern Recognition*, 142:109637, 2023.
- [8] Benjamin Recht, Maryam Fazel, and Pablo A. Parrilo. Guaranteed minimum-rank solutions of linear matrix equations via nuclear norm minimization. *SIAM Review*, 52(3):471–501, 2010.
- [9] Benjamin Recht. A simpler approach to matrix completion. *J. Mach. Learn. Res.*, 12(null):3413–3430, dec 2011.
- [10] Yudong Chen and Yuejie Chi. Harnessing structures in big data via guaranteed low-rank matrix estimation: Recent theory and fast algorithms via convex and nonconvex optimization. *IEEE Signal Processing Magazine*, 35(4):14–31, 2018.
- [11] David P. Woodruff. Sketching as a tool for numerical linear algebra. *Found. Trends Theor. Comput. Sci.*, 10(1–2):1–157, oct 2014.
- [12] Joel A Tropp and Stephen J Wright. Computational methods for sparse solution of linear inverse problems. *Proceedings of the IEEE*, 98(6):948–958, 2010.
- [13] Petros Drineas, Michael Mahoney, Senthilmurugan Muthukrishnan, and Tamas Sarlos. Faster least squares approximation. *Numerische Mathematik*, 117, 10 2007.
- [14] Prateek Jain, Praneeth Netrapalli, and Sujay Sanghavi. Low-rank matrix completion using alternating minimization. In *Proceedings of the Forty-Fifth Annual ACM Symposium on Theory of Computing*, STOC ’13, page 665–674, New York, NY, USA, 2013. Association for Computing Machinery.
- [15] Rahul Mazumder, Trevor Hastie, and Robert Tibshirani. Spectral regularization algorithms for learning large incomplete matrices. *Journal of Machine Learning Research*, 11(80):2287–2322, 2010.
- [16] Jian-Feng Cai, Emmanuel J Candès, and Zuowei Shen. A singular value thresholding algorithm for matrix completion. *SIAM Journal on optimization*, 20(4):1956–1982, 2010.
- [17] Emmanuel Candès and Benjamin Recht. Exact matrix completion via convex optimization. *Commun. ACM*, 55(6):111–119, jun 2012.

[18] Emmanuel J. Candes and Terence Tao. The power of convex relaxation: Near-optimal matrix completion. *IEEE Transactions on Information Theory*, 56(5):2053–2080, 2010.

[19] Moritz Hardt. Understanding alternating minimization for matrix completion. *2014 IEEE 55th Annual Symposium on Foundations of Computer Science*, pages 651–660, 2014.

[20] Bart Vandereycken. Low-rank matrix completion by riemannian optimization. *SIAM Journal on Optimization*, 23(2):1214–1236, 2013.

[21] Thanh Ngo and Yousef Saad. Scaled gradients on grassmann manifolds for matrix completion. In F. Pereira, C.J. Burges, L. Bottou, and K.Q. Weinberger, editors, *Advances in Neural Information Processing Systems*, volume 25. Curran Associates, Inc., 2012.

[22] Léopold Cambier and P-A Absil. Robust low-rank matrix completion by riemannian optimization. *SIAM Journal on Scientific Computing*, 38(5):S440–S460, 2016.

[23] Fengmiao Bian, Jian-Feng Cai, and Rui Zhang. A preconditioned riemannian gradient descent algorithm for low-rank matrix recovery. *SIAM Journal on Matrix Analysis and Applications*, 45(4):2075–2103, 2024.

[24] Jian-Feng Cai, Emmanuel Candès, and Zuowei Shen. A singular value thresholding algorithm for matrix completion. *SIAM Journal on Optimization*, 20:1956–1982, 03 2010.

[25] Martin Jaggi. Revisiting Frank-Wolfe: Projection-free sparse convex optimization. In Sanjoy Dasgupta and David McAllester, editors, *Proceedings of the 30th International Conference on Machine Learning*, volume 28 of *Proceedings of Machine Learning Research*, pages 427–435, Atlanta, Georgia, USA, 17–19 Jun 2013. PMLR.

[26] Robert Freund, Paul Grigas, and Rahul Mazumder. An extended frank–wolfe method with “in-face” directions, and its application to low-rank matrix completion. *SIAM Journal on Optimization*, 27, 11 2015.

[27] Alp Yurtsever, Madeleine Udell, Joel Tropp, and Volkan Cevher. Sketchy decisions: Convex low-rank matrix optimization with optimal storage. In *Artificial intelligence and statistics*, pages 1188–1196. PMLR, 2017.

[28] Samuel Burer and Renato Monteiro. Local minima and convergence in low-rank semidefinite programming. *Mathematical Programming*, 103:427–444, 07 2005.

[29] Amit Deshpande, Luis Rademacher, Santosh Vempala, and Grant Wang. Matrix approximation and projective clustering via volume sampling. *Theory of Computing*, 2:225–247, 01 2006.

[30] Petros Drineas, Michael Mahoney, and Senthilmurugan Muthukrishnan. Relative-error *cur* matrix decompositions. *SIAM Journal on Matrix Analysis and Applications*, 30:844–881, 05 2008.

[31] Danny C Sorensen and Mark Embree. A deim induced cur factorization. *SIAM Journal on Scientific Computing*, 38(3):A1454–A1482, 2016.

[32] Keaton Hamm and Longxiu Huang. Perspectives on cur decompositions. *Applied and Computational Harmonic Analysis*, 48(3):1088–1099, 2020.

[33] Sergey Voronin and Per-Gunnar Martinsson. Efficient algorithms for cur and interpolative matrix decompositions. *Advances in Computational Mathematics*, 43:495–516, 2017.

[34] Christos Boutsidis and David P Woodruff. Optimal cur matrix decompositions. In *Proceedings of the forty-sixth annual ACM symposium on Theory of computing*, pages 353–362, 2014.

[35] Michal P Karpowicz and Gilbert Strang. The pseudoinverse of $A = CR$ is $A^+ = R^+ + C^+(?)$. *arXiv preprint arXiv:2305.01716*, 2023.

[36] Keaton Hamm and Longxiu Huang. Stability of sampling for cur decompositions. *arXiv preprint arXiv:2001.02774*, 2020.

[37] Yining Wang and Aarti Singh. Provably correct algorithms for matrix column subset selection with selectively sampled data. *J. Mach. Learn. Res.*, 18(1):5699–5740, jan 2017.

[38] Armin Eftekhari, Michael B Wakin, and Rachel A Ward. MC2: a two-phase algorithm for leveraged matrix completion. *Information and Inference: A Journal of the IMA*, 7(3):581–604, 02 2018.

[39] Akshay Krishnamurthy and Aarti Singh. On the power of adaptivity in matrix completion and approximation. *CoRR*, abs/1407.3619, 2014.

[40] Akshay Krishnamurthy and Aarti Singh. Low-rank matrix and tensor completion via adaptive sampling. In C.J. Burges, L. Bottou, M. Welling, Z. Ghahramani, and K.Q. Weinberger, editors, *Advances in Neural Information Processing Systems*, volume 26. Curran Associates, Inc., 2013.

[41] Miao Xu, Rong Jin, and Zhi-Hua Zhou. Cur algorithm for partially observed matrices. In *Proceedings of the 32nd International Conference on International Conference on Machine Learning - Volume 37*, ICML’15, page 1412–1421. JMLR.org, 2015.

[42] David Gross. Recovering low-rank matrices from few coefficients in any basis. *IEEE Transactions on Information Theory*, 57(3):1548–1566, Mar 2011.

[43] HanQin Cai, Keaton Hamm, Longxiu Huang, and Deanna Needell. Robust cur decomposition: Theory and imaging applications. *SIAM J. Imaging Sci.*, 14:1472–1503, 2021.

[44] Tian Tong, Cong Ma, and Yuejie Chi. Accelerating ill-conditioned low-rank matrix estimation via scaled gradient descent. *Journal of Machine Learning Research*, 22(150):1–63, 2021.

[45] Amit Deshpande and Luis Rademacher. Efficient volume sampling for row/column subset selection. In *2010 IEEE 51st Annual Symposium on Foundations of Computer Science*, pages 329–338, 2010.

[46] Ayoub Belhadji, Rémi Bardenet, and Pierre Chainais. A determinantal point process for column subset selection. *Journal of machine learning research*, 21(197):1–62, 2020.

[47] Brendan O’Donoghue. Operator splitting for a homogeneous embedding of the linear complementarity problem. *SIAM Journal on Optimization*, 31:1999–2023, August 2021.

[48] Charles R. Harris, K. Jarrod Millman, Stéfan J. van der Walt, Ralf Gommers, Pauli Virtanen, David Cournapeau, Eric Wieser, Julian Taylor, Sebastian Berg, Nathaniel J. Smith, Robert Kern, Matti Picus, Stephan Hoyer, Marten H. van Kerkwijk, Matthew Brett, Allan Haldane, Jaime Fernández del Río, Mark Wiebe, Pearu Peterson, Pierre Gérard-Marchant, Kevin Sheppard, Tyler Reddy, Warren Weckesser, Hameer Abbasi, Christoph Gohlke, and Travis E. Oliphant. Array programming with NumPy. *Nature*, 585(7825):357–362, September 2020.

[49] Adam Paszke, Sam Gross, Francisco Massa, Adam Lerer, James Bradbury, Gregory Chanan, Trevor Killeen, Zeming Lin, Natalia Gimelshein, Luca Antiga, Alban Desmaison, Andreas Kopf, Edward Yang, Zachary DeVito, Martin Raison, Alykhan Tejani, Sasank Chilamkurthy, Benoit Steiner, Lu Fang, Junjie Bai, and Soumith Chintala. Pytorch: An imperative style, high-performance deep learning library. In *Advances in Neural Information Processing Systems 32*, pages 8024–8035. Curran Associates, Inc., 2019.

[50] Junzi Zhang, Brendan O’Donoghue, and Stephen Boyd. Globally convergent type–I Anderson acceleration for non-smooth fixed-point iterations. *SIAM Journal on Optimization*, 30(4):3170–3197, 2020.

[51] Alex Rubinsteyn and Sergey Feldman. fancyimpute: An imputation library for python.

[52] A. W. van der Vaart. *Asymptotic Statistics*. Cambridge Series in Statistical and Probabilistic Mathematics. Cambridge University Press, 1998.

[53] Paweł Szykiewicz. A comparative study of pso and cma-es algorithms on black-box optimization benchmarks. *Journal of Telecommunications and Information Technology*, 8, 01 2019.

[54] Cong Ma, Kaizheng Wang, Yuejie Chi, and Yuxin Chen. Implicit regularization in nonconvex statistical estimation: Gradient descent converges linearly for phase retrieval, matrix completion and blind deconvolution. *Foundations of Computational Mathematics*, 20, 11 2017.

[55] O. Troyanskaya, M. Cantor, G. Sherlock, P. Brown, T. Hastie, R. Tibshirani, D. Botstein, and R. Altman. Missing value estimation methods for dna microarrays. *Bioinformatics*, 17 6:520–5, 2001.

[56] F. Maxwell Harper and Joseph A. Konstan. The movielens datasets: History and context, dec 2015.

[57] Hilmi Yildirim and Mukkai S. Krishnamoorthy. A random walk method for alleviating the sparsity problem in collaborative filtering. In *Proceedings of the 2008 ACM Conference on Recommender Systems*, RecSys ’08, page 131–138, New York, NY, USA, 2008. Association for Computing Machinery.

[58] Stephen P Boyd and Lieven Vandenberghe. *Convex optimization*. Cambridge university press, 2004.

[59] Joel Tropp. Improved analysis of the subsamples randomized hadamard transform. *Advances in Adaptive Data Analysis*, 03, 11 2010.